Article ID: 1006-8775(2017) 01-0047-11

NUMERICAL SIMULATION OF THE RELATIONSHIP BETWEEN THE MAINTENANCE AND INCREASE IN HEAVY RAINFALL OF THE LANDING TROPICAL STORM BILIS AND MOISTURE TRANSPORT FROM LOWER LATITUDES

WANG Li-juan (王黎娟)[1], DAI Zhu-jun (戴竹君)[2], HE Jie-lin (何洁琳)[3]
(1. Key Laboratory of Meteorological Disaster, Ministry of Education / Joint International Research Laboratory of Climate and Environment Change / Collaborative Innovation Center on Forecast and Evaluation of Meteorological Disasters, Nanjing University of Information Science and Technology, Nanjing 210044 China;
2. Nanjing Meteorological Bureau, Nanjing 210019 China; 3. Guangxi Climate Center, Nanning 530022 China)

Abstract: The NCEP/NCAR reanalysis, Japan Meteorological Agency (JMA) tropical cyclone tracks and intensive surface observations are used to diagnose the features of moisture transport of tropical storm Bilis (No. 0604), which is simulated by the WRF (weather research and forecasting) mesoscale numerical model. It is shown that the Bilis was linked with the moisture channel in the lower latitudes after its landing. Meanwhile, the cross-equatorial flows over 80°-100°E and Somali were active and brought abundant water vapor into the tropical storm, facilitating the maintenance of the landing storm with intensified heavy rainfall along its path. The simulation suggested that the decreased water vapor from lower latitudes prevents the maintenance of Bilis and the development of rainfall. While the cross-equatorial flows over 80°-100°E and Somali were in favor of keeping the cyclonic circulation over land. If the moisture supply fro m the Somali jet stream was reduced, the strength and area of heavy rainfall in tropical cyclone would be remarkably weakened. Consequently, the decreased water vapor from lower latitudes can remarkably suppress the deep convection in tropical storm, then Bilis was damped without the persistent energy support and the rainfall was diminished accordingly.
Key words: tropical storm Bilis; moisture transport; numerical experiments; rainfall increase
CLC number: P444 **Document code:** A
doi: 10.16555/j.1006-8775.2017.01.005

1 INTRODUCTION

Based on the theory of the second conditional instability proposed by Charney, one of the important mechanisms for the Tropical Cyclone (TC) development is the turbulence amplification by the convergence in the planet boundary layer (PBL) and the upward transport of water vapor[1]. The latent heating released by the condensation of moisture warms the upper air and then decreases the low-level pressure to enhance the surface convergence, which favors the maintenance and strengthening of TC. And the TC enhancement could further facilitate the moisture transport. The two processes make up a loop of positive feedback. Thus the strong transport of water vapor is one of the major reasons for the long-duration of landing TC and the TC-induced heave storm along its path [2-4]. The essential condition for keeping the TC-induced heavy rainfall is the evident convergence of moisture, say that the abundant supply of water vapor is necessary. The TC cannot generate and maintain without sufficient transport and supply of moisture, and the mass of moisture transport and concentration is important for the formation of TC-induced heavy precipitation. Chen et al. [5] found out that the moisture supporting the TCs landing China is the equatorial air mass over the Indian Ocean or Bay of Bengal (BOB), and the tropical oceanic air mass over the South China Sea (SCS) and western North Pacific (WNP). Thus there are three major convey channels of water vapor, from the BOB, the SCS and the WNP, respectively. Besides the moisture transport from the lower latitudes exhibits evident influence on both the TC-induced precipitation and the strength and duration of TCs. The sustained transport of water vapor from lower latitudes maintains the warm core of TCs and the deep convection in the TC circulation[6-11]. Cong et al.[12] pointed out that the low-level jet stream in the south could bring energy and humid air to the TC-induced heavy storm, where the warm and wet air was converged and accumulated to increase the lower temperature and humidity, and then the atmosphere became more stratified unstable. Li et

Received 2014-05-08; **Revised** 2016-12-08; **Accepted** 2017-02-15
Foundation item: Major Program of the Natural Science Researches for Colleges and Universities in Jiangsu Province (14KJA170004);'333' Project of Jiangsu Province;National Natural Science Foundation of China (41575081, 41175061)
Biography: WANG Li-juan, professor, Ph. D., primarily undertaking research on monsoon and air-sea interactions.
Corresponding author: DAI Zhu jun, e-mail: daizhujun99@163.com

al.[13] suggested that if the landing TC was joined with a convey channel of water vapor due to the lower-layer jet stream, the TC would keep for a long time, or the TC would damp quickly. The TC without convergence of water vapor would decay fast because of no moisture support [14]. Lin et al. [15] considered that southwesterly monsoon could enhance the environmental moisture transport to change the path and the dynamical-thermal structure of TC Vongfong (No. 0214) by comparing the situation of strong and weak southwesterly monsoon. The cross-equatorial flow, as the channel of exchanging material and energy between the north and south hemisphere, is able to strengthen the transport of the water vapor from lower latitudes and the unstable energy when the flow is enhanced [16-18]. Xiao [19] pointed out a close relationship between the TC formation and the southwesterly or southerly ascribed to the overturning of cross-equatorial flow from the south hemisphere. Under the favorable background, the moisture transport and the index of cross-equatorial flow play significant roles in the occurrence of TCs[20]. The strength of cross-equatorial flow determines the water vapor converging into the TCs, which is critical for the TC duration and the intensification of heavy storm [21, 22]. However, these studies pay little attention to the association between the strength of moisture transport by cross-equatorial flow and the TC duration as well as the distribution of heavy storm[23].

The TC Bilis was sustained for a long time after its landing, and induced heavy rainfall along its path. One of the important reasons is that the abundant water vapor and unstable energy is brought into the TC circulation by the stronger monsoonal southwesterly with the onset of monsoon surge followed by the strengthening of cross-equatorial flow[14]. This paper aims to diagnose and simulate the moisture field during the landing and duration of TC Bilis by using the NCEP reanalysis dataset and the numerical model WRF 3.2.1. We will design a series of sensitivity experiments to examine the effect of moisture transport attributed to the cross-equatorial flow near 80°–100° E and 40°–60° E (Somali) on the duration of TC Bilis and the intensification of TC-induced heavy storm after its landing. On one hand, the result is useful to understanding the maintenance of TC circulation and the distribution of TC-induced heavy rainfall with the strong transport of water vapor from lower latitudes. On the other hand, they will provide more clues and ideas to the prediction of the meso- and small- scale systems in future.

2 DATA AND METHODOLOGY

The FNL global reanalysis data from NCEP/NCAR with a horizontal resolution of 1° × 1°, the reanalysis data from the ECMWF with a horizontal resolution of 2.5° × 2.5°, and the observation of Chinese automatic weather stations (AWS) are used to diagnose the transport of water vapor from lower latitudes and the strengthening of heavy rainfall induced by TC Bilis. These data are extracted from 9 to 20 July in 2006 with an interval of 6 hours. Also the records about 6-hourly best track of tropical cyclone, which is provided by Japan Meteorological Agency (JMA), are applied to describe the TC activity. And we utilize the WRF (version 3.2.1) model developed by NCEP and NCAR to simulate the evolution of TC Bilis, including its landing, duration and finally damping to a tropical low pressure. This paper addresses the influences of water vapor from lower latitudes, especially the moisture transport due to cross-equatorial flow, on both the maintenance of TC Bilis and the enhancement of TC-induced heavy storm.

3 EVOLUTION CHARACTERISTICS OF TC BILIS

3.1 *Overview of TC Bilis evolution*

The TC Bilis was formed over the ocean to the east of the Philippines on 9 July in 2006, and it landed on Yilan city of Taiwan Province at 23:00 on 13 July (Beijing time, the same below). Subsequently, it landed on the north of Fujian Province again at 12:50 on 14 July, with the max wind speed reaching storm 11 near the TC center. The TC Bilis then moved west-northwestward after its landing, and weakened to be a tropical storm in the afternoon of 14 July. Afterwards it was damped to tropical depression over the southwestern Jiangxi Province in the afternoon of 15 July, and finally diminished over the eastern Yunnan Province. The TC Bilis was maintained for 5 days after its landing, and induced heavy rainfall and extraordinary storm over the southern Zhejiang Province, the eastern and southern Fujian Province, the southern Jiangxi Province, the northern and eastern Guangdong Province. After its landing, the TC Bilis was joined with a southwesterly jet stream in the lower troposphere for a long time because of the strong cross-equatorial flow bringing rich moisture into the TC. Thus the TC Bilis was decaying slowly with the long-duration complete cyclone circulation[24]. Generally, the heavy rainfall takes place near or to the north of the TC center, as well as the inverted trough to the northeast of the TC center after its landing [25]. But the heavy storm yields to the south of TC Bilis after the landing. After the TC Bilis landed on Taiwan, the strong rainfall, which is ascribed to the TC cloud structure, occurred over the southern Zhejiang, the southeastern Fujian Province, and the joint district between the two provinces before it landed on Fujian Province. The heavy rainfall was located to the north of TC center. While the monsoon surge started at 02:00 on 15 July, the heavy storm occurred over the joint region among Guangdong, Hunan and Jiangxi Province and the eastern Guangdong Province. The rainfall was intensified with its center moving to the south of TC center.

3.2 *Transport of water vapor during the TC landing*

The moisture flux at 850 hPa shows that the water vapor comes from the SCS at 14:00 on 14 July before the landing of TC Bilis, accompanied by a weak southwesterly moisture convey belt over the Indochina Peninsula (Fig.1a). At 02:00 on 15 July, a broad and strong convey belt of moisture flux was passing through the Arabian Sea, the BOB, the Indochina Peninsula and the SCS, to the southern China (Figure.1b). The difference of 850-hPa wind field between 14:00 on 14 July and 02:00 on 15 July (Figures ignored) points out that both the Somali jet and the cross-equatorial flow near 80°–100°E was enhanced evidently at 02:00 on 15 July, presenting a wide-ranging southwesterly from the Arabian Sea to the southern China. This is a mark of monsoon surge onset[26]. Hence the broad moisture convey belt was collaborated with the cross-equatorial flow and the monsoon surge. Specifically, the sufficient moisture was transported to the southern China with the enhanced Somali jet and the cross-equatorial flow near 80° –100° E and the monsoon surge onset. Then the maximum of moisture flux exceeds 50g/(cm·hPa·s) to the southeast of TC Bilis center, consistent with the intensified torrential rainfall to the south of the TC. At 08:00 on 18 July, this moisture convey belt was weakened but still sustained to transport the water vapor to southern China, with a center of moisture flux reaching 25 g/(cm·hPa·s) settled over Guangxi Province (figures ignored). This moisture convey belt did not disappear until 20:00 on 18 July when the TC Bilis was diminishing (figures ignored), implicating that the long-duration of TC Bilis was primarily attributed to the mass water vapor brought into the TC circulation by the strong southwesterly over the Indian Ocean and the BOB and the evident cross-equatorial flow.

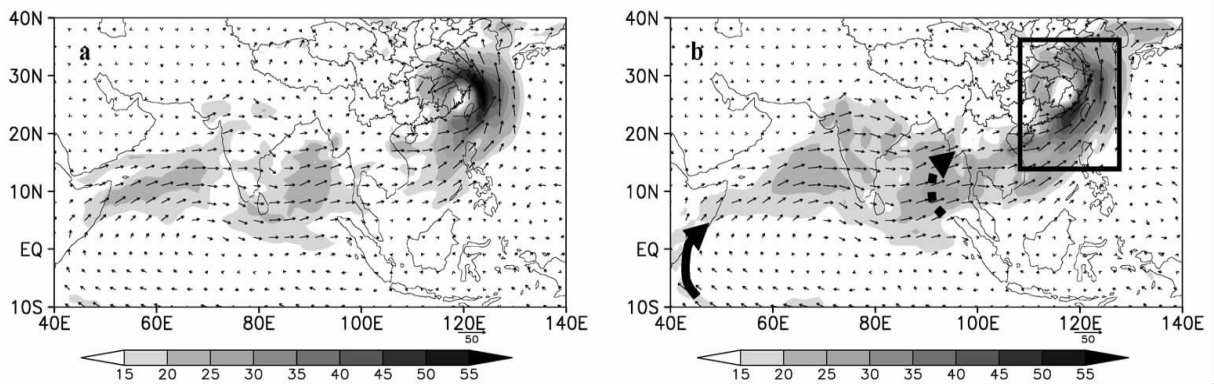

Figure 1. Horizontal distribution of 850-hPa moisture flux at (a) 14:00 on 14 July and (b) 02:00 on 15 July (units: g/(cm·hPa·s)). Shading is for the moisture flux greater than 15 g/(cm·hPa·s). The solid and dashed arrow in (b) is for the enhancement of moisture transport by the Somali Jet stream and the cross-equatorial flow over 80°–100°E, respectively.

Figure 2 is the vertical profile of moisture flux on the four edges around the TC Bilis (110°–130°E, 16°–37° N) when the monsoon surge onset. The heavy lines in Fig. 1b mark the four edges, respectively. Here the moisture flux into each edge is defined as positive, and the formula of moisture flux on the western, eastern, southern and northern edge is qu/g, $-qu/g$, qv/g and $-qv/g$, respectively. It is demonstrated that the moisture transport is limited under 700 hPa, and the maximum of moisture inflow is to the south of western edge at 850 hPa (Fig.2a). Besides the moisture outflow is strongest at 850 hPa. The moisture inflow on the southern is much stronger than the outflow on the northern edge. The moisture flux on the eastern edge enters the TC from the south on the lower levels, and then leaves the TC on the north in the mid-lower troposphere (Fig. 2b). The moisture flux comes into the TC with no outflow on the southern edge with the maximum of 35 g/(cm·hPa·s) at 1,000 hPa, which is only less the max moisture flux of 42 g/(cm·hPa·s) on the western edge. On the northern edge, only is there moisture outflow from the TC with a maximum of -30 g/(cm·hPa·s) at 900 hPa (Fig.2d). As a result, the moisture inflow is much larger than its outflow through the edges of TC center.

3.3 *Stream function and velocity potential of moisture flux*

The non-divergent stream function of moisture flux, i.e. the non-divergent moisture flux, represents the moisture transport along the isobars, which is the primary component of global moisture convey. While the divergent moisture flux is the component crossing the isobars. Although the divergent component is small for the global moisture transport, it is important for the source and sink of water vapor [27]. Therefore, the stream function reflects the moisture transport, whereas the velocity potential could explain the possible reason for the maintenance of moisture content[28]. Then we can understand the role of moisture variation in the movement and lifecycle of TC by investigating the large-scale moisture transport and long-duration divergence and convergence of water vapor during the genesis, development, movement and decaying of TC Bilis. Here the ECMWF global reanalysis with a

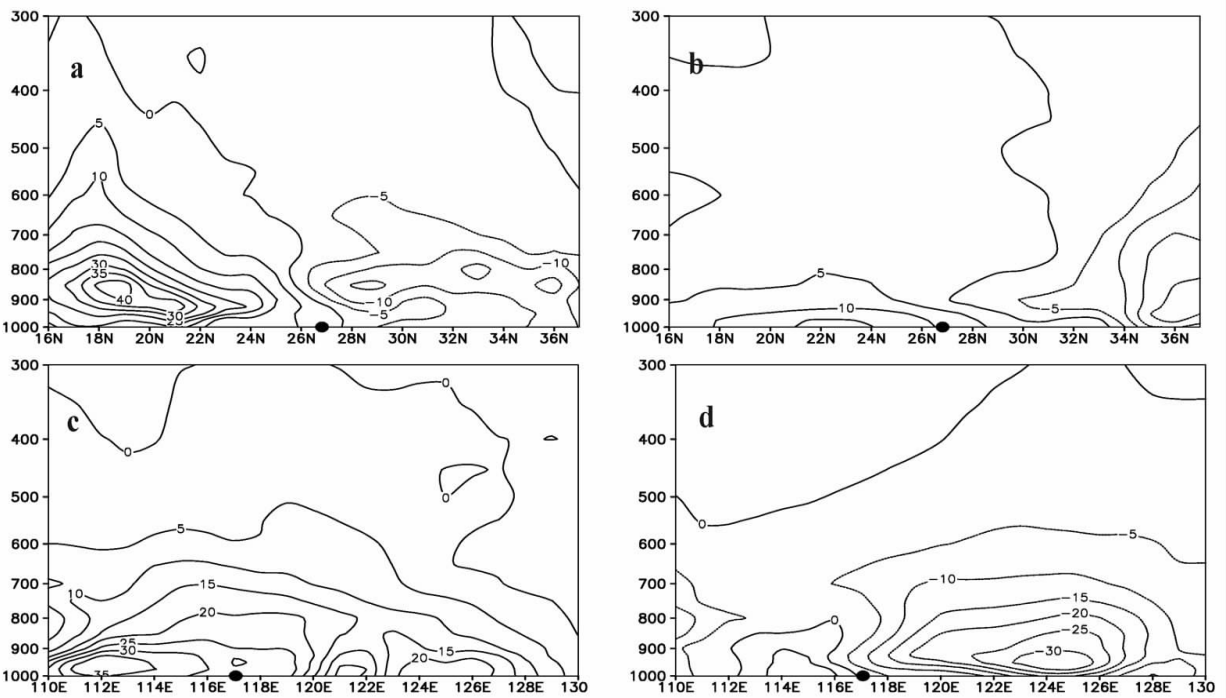

Figure 2. Vertical profile of moisture flux on the southern, eastern, southern, northern edge of the region (110°–130°E, 16°–37°N) at 02:00 on 15 July (units: g/ (cm·hPa·s)). Dots are for the longitude of TC Bilis center, the same below. The inflow and outflow on each edge is defined as positive and negative, respectively.

horizontal resolution of 2.5°× 2.5° is applied to examine the large-scale circulation of moisture. The variables in this dataset are distributed on 11 isobaric surfaces from 1,000 to 100 hPa, and are output 4 times per day (i.e., 00:00, 06:00, 12:00, and 18:00 UTC).

Figure 3a displays the horizontal distribution of averaged stream function and velocity potential of moisture flux during the whole lifecycle of TC from its formation to extinction. It is shown that three maximum centers of stream function in the Northern Hemisphere are located over the Indian Monsoon region, the Pacific and the Atlantic, respectively. Firstly, the water vapor over the Pacific is transported westward to the south of WNP by the equatorial easterly. Then part of the moisture is brought northward to the SCS and further to the coast of southern China, while another part is moving westward to the Somali and crossing the equator to the BOB. Some of the latter is carried northeastward into southern China. Thus the moisture transport by the cross-equatorial flow near Somali and 80°–100° E is remarkable during the lifecycle of TC Bilis.

The velocity potential and divergent component of moisture flux in the meantime are portrayed in Fig. 3b, which shows a negative center of velocity potential over the region from eastern Eurasian continent to central Pacific. During the appearance of TC Bilis, the most evident sink of water vapor is situated over the area from eastern China to western Pacific, where the humid air is converged from the southwestern, the southeastern and the northwestern direction. And in the negative center of velocity potential, the moisture is transported from the Indian Ocean via the BOB and SCS to southern China, where the meridional convergence of water vapor is dominant.

4 DESIGNATION OF NUMERICAL EXPERIMENTS AND THEIR RESULTS

4.1 *Experimental design*

The diagnosis indicates that the strong cross-equatorial flow could transport mass of moisture and energy to the circulation of TC Bilis after its landing. Then the TC could maintain for a long time with the water vapor conveyed from the lower latitudes, especially from the cross-equatorial flow. The TC-induced rainfall is increased after the TC landing with the strongest rainstorm settled to the south of TC center, rather than near the center as usual[29]. Then what is the association between the strong transport of moisture from lower latitudes and the distribution of rainstorm as well as the long-duration of TC Bilis after its landing? How does the weakened moisture transport by the cross-equatorial flow influence the maintenance of TC Bilis and the distribution of rainstorm? These questions will be answered by a series of numerical experiments.

The hydrostatic meso-scale numerical model WRF (version 3.2.1) is adopted to simulate the landing process of TC Bilis. The initial field for this model is the NCEP/NCAR FNL reanalysis dataset with a horizontal resolution of 1°× 1°. The double-fold nesting and a Mercator projection are adopted with the regional

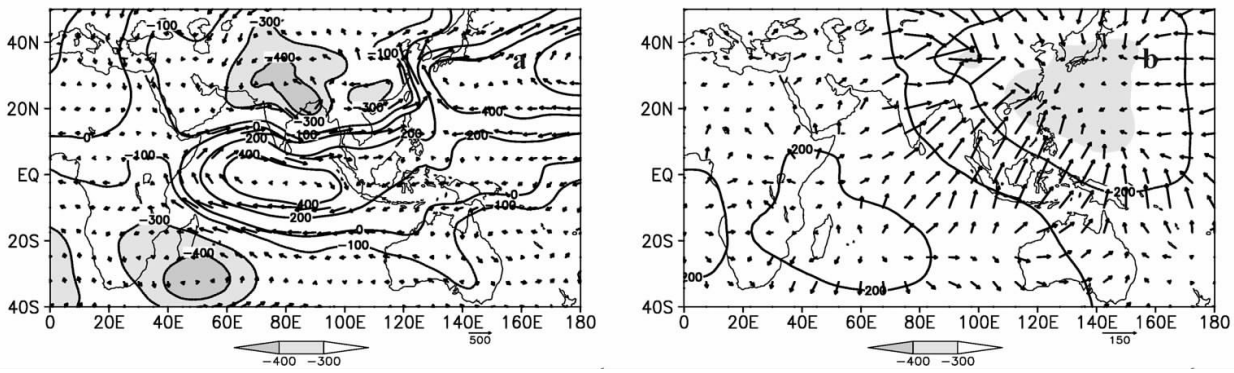

Figure 3. Averaged (a) stream function (contours, units: 10^6 kg/s) and (b) velocity potential (contours, units: 10^6 kg/s) of vertically-integrated moisture flux in the whole troposphere (1,000–300 hPa) from 9 to 18 July. The vectors in (a) and (b) are for the non-divergent and divergent component of moisture flux (units: kg/(m·s)), respectively.

center over (91°E, 15°N) (Fig. 4). The grid distance of coarse mesh (Mesh 1) is 45 km with grid numbers of 251× 151, whereas the that of fine mesh (Mesh 2) is 15 km with grid numbers of 361 × 244. The horizontal resolution of topographic data is 10 and 5 min in the coarse and fine mesh, respectively. The 38 levels are non-homogeneous in vertical, and the total integration time is 54 h with a time step of 90 s. The simulation starts at 20:00 on 13 July to 02:00 on 16 July, including the period when the TC Bilis lands, maintains, and even weakens to a tropical depression. There are many parameterization schemes for PBL, cloud-radiation, micro-physical procedure and cumulus convection in WRF, and the selection of the schemes is vital for the simulation [28-32]. After comparing many simulations based on different groups of schemes, we select one of them, which are listed in Table 1, to conduct the experiments. And the simulation with the selected schemes is treated as the control run (CTL).

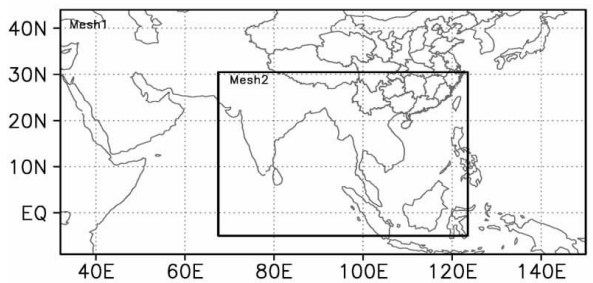

Figure 4. Region of the coarse (Mesh 1) and fine (Mesh 2) mesh in WRF.

Table 1. Parameterization schemes in the simulation.

Parameterization schemes	Coarse mesh (Mesh1)	Fine mesh (Mesh2)
Micro-physical process	Kessler	Wsm5
Cumulus convection	Betts-Miller-Janjic	Grell-3D
Land process	Unified Noah land-surface	Unified Noah land-surface
PBL	YSU scheme	YSU scheme
Radiation process	LW :RRTM	LW :RRTM
	SW :Dudhia	SW :Dudhia

4.2 *CTL results*

Figure 5 shows the center position and path of TC Bilis in JMA observation and WRF simulation. The simulated TC center is 71 km away from the observation in average from 20:00 on 13 July every 6 hours. The simulated path is no more than 1 degree to the north of observation. And the deviation of simulation is closing to the observation with time. In particular, the simulation matches well with the observation at 02:00 on 15 July when the monsoon surge onset. Therefore, the WRF is able to simulate the path of TC Bilis.

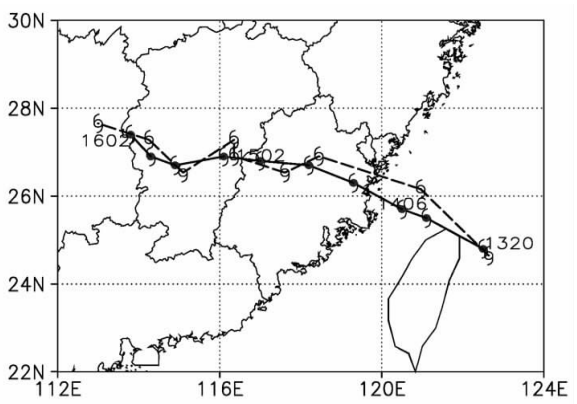

Figure 5. The path of TC Bilis from 20:00 on 13 July to 08:00 on 16 July in simulation (dashed line) and observation (solid line, JMA data).

In addition, the magnitude and variation of TC Bilis strength is also represented by WRF (Fig. 6). In the beginning of simulation, the simulated sea level pressure (SLP) near the TC center is 6 hPa weaker than the observation, which may be ascribed to the weaker TC strength in the NCEP/NCAR FNL reanalysis. Afterwards the WRF could well simulate the weakening trend of TC strength. The value and variation of SLP in CTL is well consistent with that in observation after 20:00 on 14 July. Generally, the path and strength variation of TC Bilis in the WRF simulation could catch the primary features of the observation.

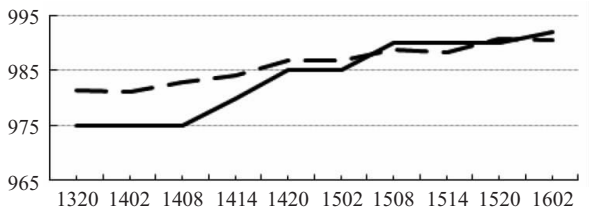

Figure 6. Sea level pressure near the center of TC Bilis in simulation (dashed line) and observation (solid line). The abscissa is for the Beijing time, and the ordinate is for the SLP values (units: hPa).

After the TC Bilis lands on Taiwan Island and before it lands on Fujian Province, the WRF could well simulate the rainstorm located over the joint area between Zhejiang and Fujian Province, i.e., to the south of Taiwan Island (Fig.7a), but the rainfall in simulation is a little weaker than that in observation (Fig.7b). After the TC Bilis lands on Fujian Province, the two heavy rainfall centers situated over the joint area between Hunan and Guangdong and the eastern Guangdong Province are well simulated from 02:00 on 15 July to 02:00 16 July when the monsoon surge onset (Figs.7c and 7d). The area of simulated rainfall over the joint region between Hunan and Jiangxi Province is larger than the observation, and the precipitation center is 220 mm, which is a little weaker than the observation of 240 mm. The simulated rainfall on the south of Guangdong Province is to the east of the observed one, and its strength is a little weaker than the observation. Overall, the WRF could simulate the asymmetric distribution of rainfall and the southward shifting of rainstorm from the TC center to its south before and after the landing of TC Bilis.

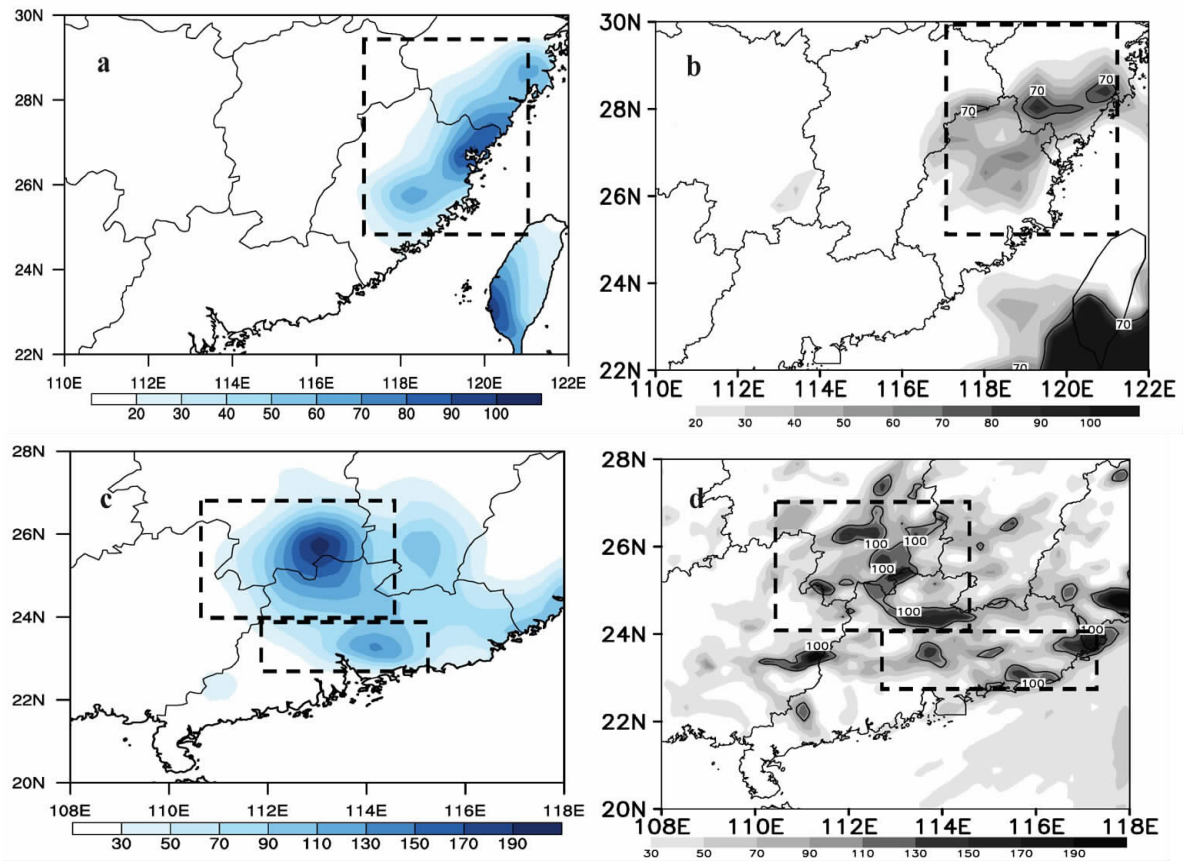

Figure 7. Accumulated rainfall amount in (a, c) simulation and (b, d) observation averaged (a, b) from 20:00 13 July to 14:00 14 July and (c, d) from 02:00 15 July to 02:00 16 July. Units: mm.

The 6-hourly simulated precipitation exhibits the increase of rainfall with the monsoon surge onset from 06:00 on 14 July to 18:00 on 15 July, as shown in observation (figures ignored). It is indicated by Figs.5 to 7 that the CTL by WRF model is successful in simulating the path, strength and rainfall of TC Bilis, especially the rainstorm development after monsoon surge onset at 02:00 on 15 July is well simulated. Thus the result of CTL is reliable.

4.3 *Sensitivity experiments of moisture*

The background of moisture transport indicates that the water vapor coming from lower latitudes, especially carried by cross-equatorial flow, is important for the long-duration of TC Bilis and the rainstorm enhancement after the TC landing. It is still unclear which convey belt of water vapor controls these processes. Then a series of sensitivity experiments with respect to moisture are designed to investigate the

relative effect of water vapor from different source on the TC duration and rainstorm development. Here we change the moisture convey coming from the cross-equatorial flow over (80°–100°E, 10°S–10°N) and the Somali jet stream over (40°–60°E, 10°S–10°N) to reveal the dominant source of water vapor. Since the fine mesh (68°–123°E, 5°S–30°N) dose not cover the Somali jet stream, only the low-layer (1,000–850 hPa) specific humidity (QVAPOR, units: kg/kg) in the coarse mesh is changed in the CTL run to conduct the sensitivity experiments as follows.

(1) NEQU run: the lower-level specific humidity over (80°–100°E, 10°S–10°N) and (40°–60°E, 10°S–10°N) are weakened to 30% of their original values every 6 hours in the coarse mesh.

(2) NEQUd01 run: The specific humidity over (80°–100°E, 10°S–10°N) is decreased 70% every 6 hours in the coarse mesh.

(30) NSMJd01 run: The same as NEQUd01 run, but the decreased specific humidity is over (40°–60°E, 10°S–10°N) instead.

4.3.1 RESPONSE OF WATER VAPOR FIELD

The weakening of water vapor is described by subtracting the specific humidity of CTL run from that of sensitivity runs. The smaller value of specific humidity difference field implies more evident damping of water vapor in sensitivity runs. Fig.8 shows the difference of specific humidity at 850 hPa between sensitivity and CTL run after integrating for 42 hours. It also presents the accumulated difference of 850-hPa specific humidity between sensitivity and CTL run from 02:00 on 15 July to 02:00 on 16 July. The former suggests that the specific humidity in the three sensitivity runs is all decreased after 42 hr integration (shading, Figs.8a to c). In detail, the specific humidity is attenuated prominently on the west of TC center in the NEQU and NSMJd01 runs, whereas the decreasing is weak in NEQUd01 run. The accumulated difference of specific humidity from 02:00 on 15 July to 02:00 on 16 July presents the strong attenuation on the west of TC center in NEQU and NSMJd01 runs, but weak and scattered anomalies in NEQUd01 run (Figs.8d to f). The result proposes that the reduction of water vapor in the cross-equatorial flow in coarse mesh, especially the Somali jet stream (40° –60° E), could effectively decrease the moisture transport and the water vapor in the TC circulation. Consequently, the moisture transported by the cross-equatorial flow near Somali is important for the duration of TC Bilis after its landing.

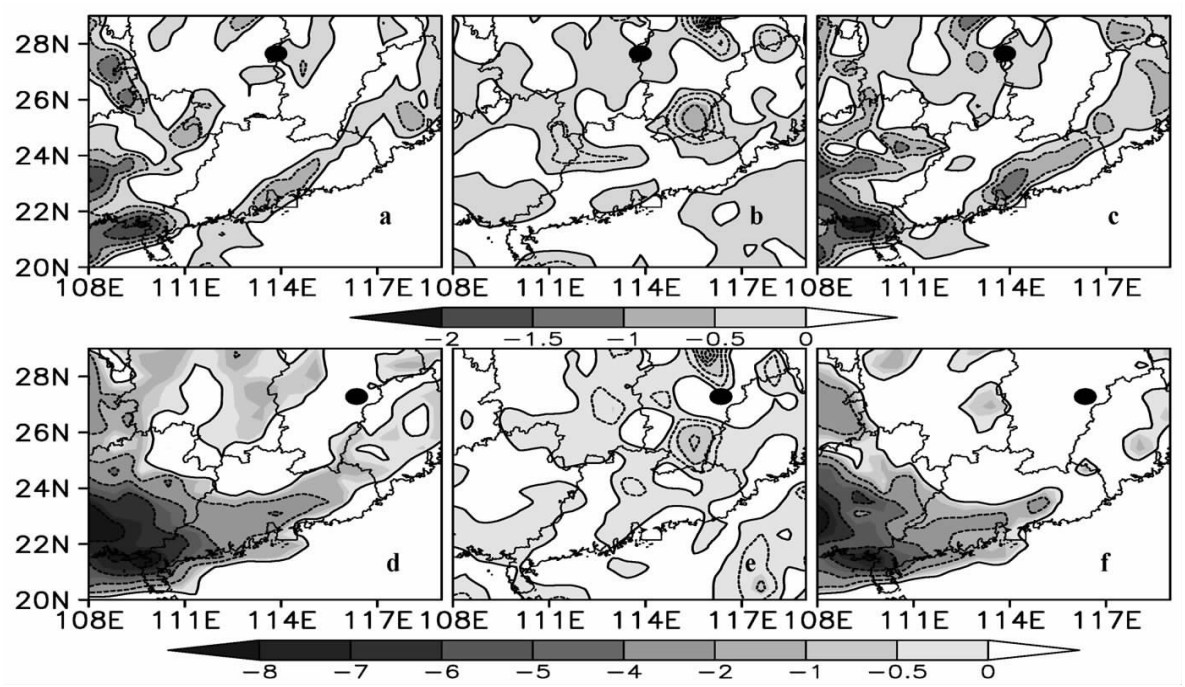

Figure 8. The reduction of 850-hPa specific humidity in the sensitivity runs (a-c is for the results after 42hr integration, d-f is for the accumulated value from 02:00 on 15 July to 02:00 on 16 July). Dot represents the position of TC center in CTL run (same as below). (a), (d): NEQU run; (b), (e): NEQUd01; (c), (f): NSMJd0.

4.3.2 RESPONSE OF ATMOSPHERIC CIRCULATION

The differences of wind at 850 hPa between sensitivity and CTL run are used to examine the influence of decreased moisture on the cyclone decaying. The differences are obtained by subtracting the CTL output from the sensitivity results. The anticyclone in difference fields is proportional to the decaying of TC cyclonic circulation in the sensitivity runs. The difference of 850-hPa circulation in NEQU, NEQUd01, and NSMJd01 after 42 hours integration is shown in Fig.9. The anomalous anticyclone is evident near the TC Bilis center in the three sensitivity runs,

implicating that the TC cyclonic circulation is damped by the weaker moisture transport. The landing TC is sensitive to the environmental moisture transport. Specifically, the anomalous anticyclone is strong in NEQU and NSMJd01 runs (Figs.9a and 9c) but weak in NEQUd01 run (Fig.9b). The weak anticyclone anomaly is located to the southwest of TC center with much smaller strength and density of anomalous wind in NEQUd01 run. Then the decaying of TC circulation in NEQUd01 run is slower than that in either NEQU or NSMJd01 run. As a result, the influence of decreased water vapor in the cross-equatorial flow over 80°–100°E on the maintenance of TC Bilis is less than that induced by dry anomaly in the Somali jet stream.

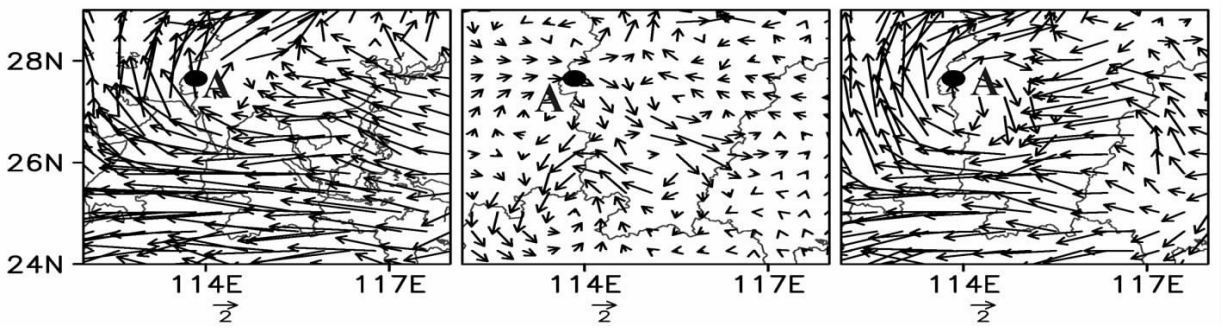

Figure 9. Difference of 850-hPa circulation in the (left panel) NEQU, (middle panel) NEQUd01, and (right panel) NSMJd01 runs after 42-hr integration compared with CTL run (units: m/s). "A" is for the position of anticyclone anomaly.

The results suggest that the TC circulation will maintain after its landing if it obtains moisture from the environment. The background moisture transport, especially by the cross-equatorial flow over Somali, is important for the TC duration. While the effect of moisture transported by the cross-equatorial flow over 80°–100°E is lesser on the maintenance of TC Bilis.

4.3.3 RESPONSE OF TC-INDUCED RAINFALL

The moisture conveys are important for the development of TC-induced rainstorm. Figure 10 presents the precipitation within 24 hours (02:00 on 15 July to 02:00 on 16 July) after monsoon surge onset in NEQU, NEQUd01 and NSMJd01, respectively. Since the specific humidity has only been changed in coarse mesh, we have to examine the rainfall response in both coarse (Figs.10a to c) and fine (Figs.10d to f) meshes. The result in coarse mesh could depict a more comprehensive picture of TC-induced rainfall under the influence of different moisture transport situation. The outputs verify that the rainfall is decreased dramatically in NEQU and NSMJd01 runs with weak precipitation over the joint area between Hunan and Jiangxi Province. It is indicated that the reduction of moisture transport in NEQU and NSMJd01 runs could evidently decrease the rainfall amount of the two rainstorm centers after the TC landing. In NEQUd01 run, although the decreased moisture transport from cross-equatorial flow over 80°–100°E could suppress the rainstorm over the joint area between Hunan and Jiangxi and the southern Guangdong Province, the effect is limited, presenting that the accumulated rainfall amount is more than 40 mm over the joint area between Hunan and Jiangxi Province and above 30 mm over the southern Guangdong Province. Note that the strength of rainfall in NEQUd01 run is weaker than that in CTL run (Fig. 7d). The rainfall amount and area on fine mesh in the three sensitivity runs is weaker than that in CTL run, implicating the direct impacts of environmental moisture transport on the magnitude and area of rainstorm development after the TC landing. Also the accumulated rainfall amount in NEQUd01 run (Fig. 10e) exceeds 160 mm over the joint area between Hunan and Jiangxi Province, while the counterparts in NEQU and NSMJd01 runs (Fig. 10d and 10f) are 100 mm.

Figure 10 illustrates that the moisture coming from different sources can influence the strength and area of TC-induced rainfall. In NSMJd01 run, the TC-induced rainfall is evidently weakened with shrinking area when the moisture transport is attenuated. And the decaying effect in NEQUd01 on the TC-induced rainfall is less significant than that in either NEQU or NSMJd01 run, verifying the important role of moisture transported by the cross-equatorial flow over Somali in the rainstorm development after the TC landing. Meanwhile, the contribution of moisture carried by cross-equatorial flow over 80°–100°E is relatively small.

The distribution of radar echoes in different sensitivity runs could also reflect the effect of moisture transport from different sources on the convection in the TC circulation. Fig.11 is the difference of radar echoes and wind at 850 hPa in the sensitivity runs comparing with those in CTL run after the 42-hr integration. The results show that the echoes are damped in a spiral pattern near the TC Bilis circulation in all the three sensitivity runs, indicating that the decreased moisture transport could evidently prevent the convection in TC circulation. However, the damped radar echoes are asymmetrically distributed in the specific sensitivity run. In the NEQU and NSMJd01 runs, the damped echoes are located to the southwest of TC cyclonic circulation, consistent with the diminished rainstorm over the joint area of Hunan, Jiangxi and Guangdong Province (Figs.

11a and c). The strength and coverage of damped echoes in the NEQUd01 run is much smaller so that the effect of decreased moisture transport from cross-equatorial flow over 80°–100°E is weaker on the TC convection (Fig.11b). Hence the convection is suppressed near the TC circulation in NEQU, NEQUd01 and NSMJd01 runs. Then the latent heating released by condensation is decreased to inhibit the maintenance of warm core in TC and TC-induced rainfall, corresponding to the evident attenuation of TC wind and precipitation (Figs. 10 and 11).

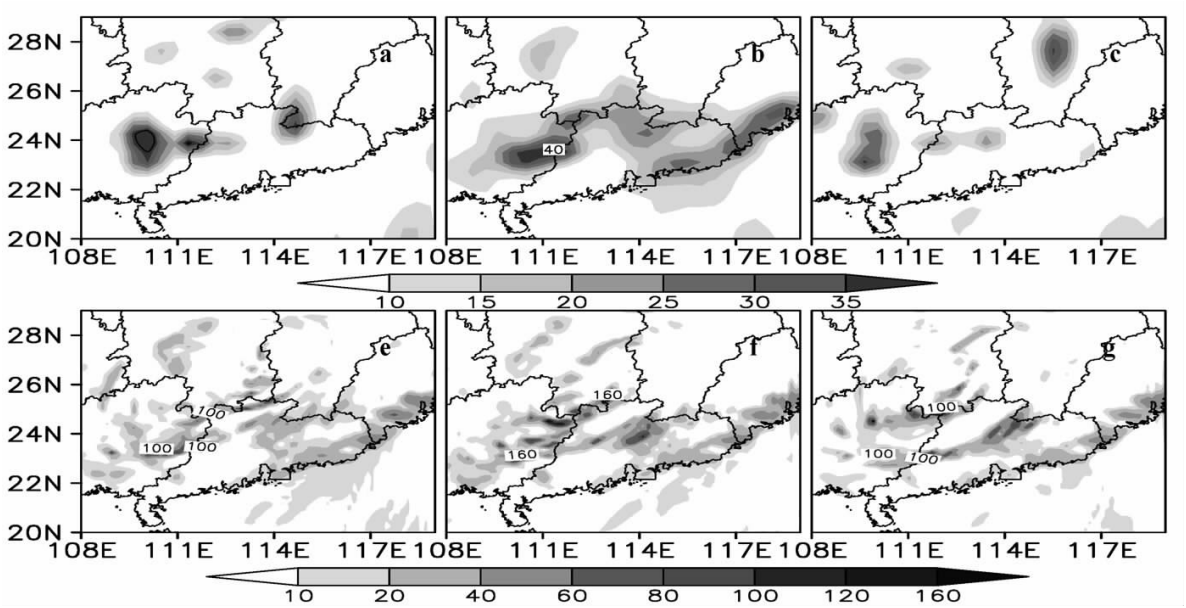

Figure 10. Accumulated rainfall amount on coarse (a to c) and fine (d to e) mesh from 02:00 on 15 July to 02:00 on 16 July in the three sensitivity runs (units: mm). (a), (d): NEQU run; (b), (e): NEQUd01; (c), (f): NSMJd01.

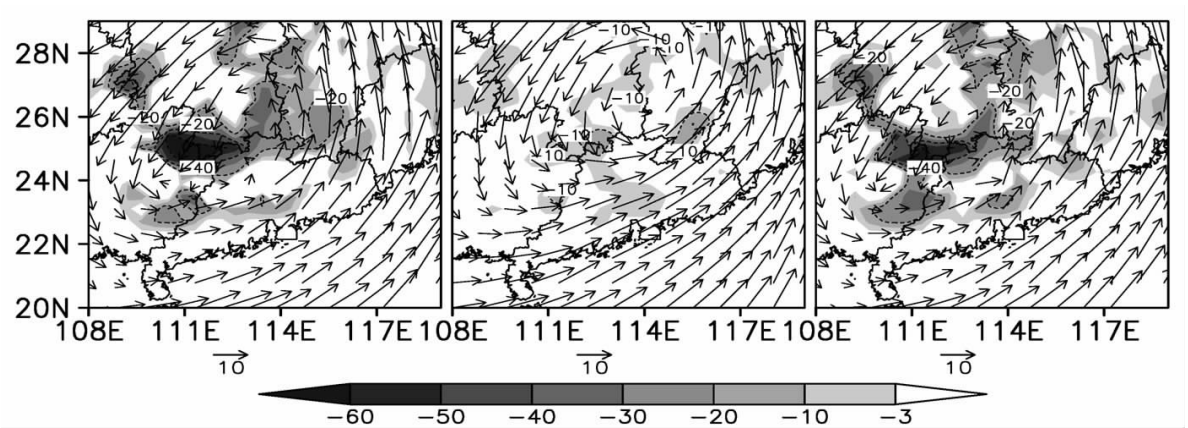

Figure 11. Difference of wind (vectors, units: m/s) and radar echoes (shading, units: dbz) at 850 hPa in sensitivity runs comparing with that in CLT run after 42-hr integration. (left panel): NEQU run; (middle panel): NEQUd01; (right panel): NSMJd01.

5 CONCLUSIONS

(1) The landing of TC Bilis encounters the development of monsoonal southwesterly and cross-equatorial flow, which brings warm and wet air into the TC circulation. Then the TC could maintain for a longtime after its landing, and the TC-induced rainstorm is flourishing with the rich supply of water vapor and heat energy. Before the monsoon surge onset, the moisture primarily comes from the SCS. After the establishment of monsoon surge, the southwesterly monsoon and the cross-equatorial flow brings abundant moisture to the TC circulation from the Indian Ocean and the BOB.

(2) The WRF model could well simulate the path and strength of TC Bilis. The cross-equatorial flow over Somali and 80°–100°E provides persistent supplement of water vapor to facilitate the long-duration of TC Bilis after its landing. The environmental moisture transport, especially that from cross-equatorial flow over Somali, is able to slow the decaying of cyclonic circulation in the landed TC. Meanwhile, the influence of moisture transported by the cross-equatorial flow over 80°-100°E on the maintenance of landed TC Bilis is weaker.

(3) The intensity and area of TC-induced rainfall is strongly impacted by the strength of moisture supply in the background. The moisture carried by the cross-equatorial flow over both 80°–100°E and Somali is in favor of the increase of rainstorm in the TC circulation. And the contribution of the latter is stronger than the former.

(4) The persistent moisture transport is conducive to the convection development in the TC Bilis. If the moisture transport is decreased, especially that by the cross-equatorial flow over Somali, the condensation heating released by convection in the TC will be weakened. Subsequently the deep convection in TC Bilis will be damped.

Acknowledgement: We are truly grateful to two anonymous reviewers for providing professional comments and suggestions to this study. We are also thankful to Dr. LI Hao-rui, from Guangzhou Institute of Tropical and Marine Meteorology Institute, China Meteorological Administration, for offering insightful assistance during the early stage of this research.

REFERENCES:

[1] CHARNEY J G, ELIASSEN A. On the growth of the hurricane depression [J]. J Atmos Sci, 1964, 21(1): 68-75.

[2] CHEN Lian-shou, MENG Zhi-yong. An overview on tropical cyclone research progress in China during the past ten years [J]. Chin J Atmos Sci, 2001, 25(3): 420-432 (in Chinese).

[3] CHEN Lian-shou, LUO Zhe-xian, LI Ying. Research advances on tropical cyclone landfall process [J]. Acta Meteorol Sinica, 2004, 62(5): 541-549 (in Chinese).

[4] LI Ying, CHEN Lian-shou. Numerical study on impact of the boundary layer fluxes over wetland on sustention and rainfall of landfalling tropical cyclones [J]. Acta Meteorol Sinica, 2007, 21(1): 34-46 (in Chinese).

[5] CHEN Lian-shou, DING Yi-hui. Introduction to Typhoons over the Western Pacific [M]. Beijing: Science Press, 1979: 443 (in Chinese).

[6] DING Yi-hui, LIU Yue-zhen. Study on the moisture budget in the No.7507 Typhoon [J]. Acta Oceanol Sinca, 1986, 8 (3): 291-301 (in Chinese).

[7] LI Ying, CHEN Lian-shou, XU Xiang-de. Numerical experiments of the impact of moisture transportation on sustaining of the landfalling tropical cyclone and precipitation [J]. Chin J Atmos Sci, 2005, 29(1): 91-98 (in Chinese).

[8] CHEN Hua. Downstream development of baroclinic waves in the midlatitude jet induced by extratropical transition: A case study [J]. Adv Atmos Sci, 2015, 32(4): 528-540.

[9] CHEN Hua, PAN Wei-yu. Denial experiments of targeted observations for extra-tropical transition of hurricane Fabian: Signal propagation, the interaction between Fabian and mid-latitude flow, and observation strategy [J]. Mon Wea Rea, 2010, 138(8): 3324-3342.

[10] GUAN Zhao-yong, LU Chu-han, MEI Shi-long, et al. Seasonality of interannual inter-hemispheric oscillations over the past five decades [J]. Adv Atmos Sci, 2010, 27 (5): 1 043-1 050.

[11] HUANG Xiao-yan, GUAN Zhao-yong, HE Li, et al. A PNN prediction scheme for local tropical cyclone intensity over the South China Sea [J]. Nat Hazards, 2016,81(2): 1249-1267.

[12] CONG Chun-hua, CHEN Lian-shou, LEI Xiao-tu, et al. An overview on the study of tropical cyclone remote rainfall [J]. J Trop Meteorol, 2011, 27 (2): 264-270 (in Chinese).

[13] LI Ying, CHEN Lian-shou, WANG Ji-zhi. The diagnostic analysis on the characteristics of large scale circulation corresponding to the sustaining and decaying of tropical cyclone after its landfall [J]. Acta Meteorol Sinica, 2004, 62(2): 167-179 (in Chinese).

[14] WANG Li-juan, GAO Hui. Diagnosis and numerical simulation of increased torrential rainfall associated with a landfalling typhoon coupled with southwest monsoon [J]. Trans Atmos Sci, 34(6): 662-671.

[15] LIN Ai-lan, WAN Qi-lin, LIANG Jian-yin, et al. Influence of tropical southwest monsoon on tropical cyclone Vongfong (0214) [J]. Acta Meteorol Sinica, 2004, 62(6): 841-850 (in Chinese).

[16] LU Chu-han, GUAN Zhao-yong, Li Yong-hua, et al. Interdecadal linkages between the Pacific decadal oscillation and interhemispheric air mass oscillation and their possible connections with East Asian Monsoon [J]. Chin J Geophys, 2013, 56(2): 117-128.

[17] JIN Da-chao, GUAN Zhao-yong, CAI Jia-xi, et al. Interannual variations of regional summer precipitation in mainland China and their possible relationships with different teleconnections in the past five decades [J]. J Meteorol Soc Jpn, 2015, 93(2): 265-283.

[18] LI Ming-gang, GUAN Zhao-yong, JIN Da-chao, et al. Anomalous circulation patterns in association with two types of daily precipitation extremes over southeastern China during boreal summer [J]. J Meteorol Res, 2016, 30(2): 183-202.

[19] XIAO Weng-jun. Preliminary investigation on the association between the cross-equatorial flow and the occurrence of Typhoon in 1982 [J]. Acta Oceanol Sinca, 1987, 9(1): 115-120 (in Chinese).

[20] HUANG Jiang-ling. Influences of cross-equatorial flow on the Typhoon and the tropical depression[J]. J Jimei Univ, 1997, 2(2): 34-38 (in Chinese).

[21] HU Ding-zhu, TIAN Wen-shou, Guan Zhao-yong,et al. Longitudinal asymmetric trends of tropical cold-point tropopause temperature and their link to strengthened Walker Circulation [J]. J Climate, 2016, 29: 7755-7771.

[22] JIN Zhen-hua, GUAN Zhao-yong. Climatological lowfrequency oscillation of OLR over the maritime continent with its possible linkage to summer precipitation in China [J]. J Trop Meteorol, 2015, 21(4): 361-373.

[23] WANG Hong-xia, WANG Li-juan, HE Jin-hai. Advances researches on cross-equatorial flows [J]. Meteorol Disast Reduct Res, 2010, 33(2): 15-18 (in Chinese).

[24] HUANG Yong, LI Chong-yin, WANG Ying. Study on the causation of anomaly of cyclogenesis frequency and location of tropical cyclones over the western north Pacific in 2006 [J]. J Trop Meteorol, 2008, 24 (6): 590-598.

[25] XU Ying-long, GAO Quan-zhu, LIU Zhen-kun. Analysis on the possible reason for the maintenance of the landing TC "Yunna" [J]. Meteorol Mon, 2005, 31(5): 32-36.

[26] Editorial committee of Atmospheric Science Thesaurus. Atmospheric Science Thesaurus [M]. Beijing: China Meteorological Press, 1994: 1-980 (in Chinese).
[27] DENG Guo, ZHOU Yu-shu, YU Zhan-jiang. Analysis of water vapor transportation in typhoon Dan (9914) [J]. J Trop Meteorol, 2005, 21(5): 533-541.
[28] JIANG Zhi-hong, LIANG Zhuo-ran, Liu ZHENG-yu, et al. A diagnostic study of water vapor transport and budget during heavy precipitation over the Huaihe river basin in 2007 [J]. Chin J Atmos Sci, 2011, 35 (2): 361-372 (in Chinese).
[29] YU Zhen-shou, CHEN Min, YE Zi-xiang, et al. Analysis of rainstorm associated with similar track tropical cyclones 'HAITANG' (0505) and 'BILIS' (0604) [J]. J Trop Meteorol, 2009, 25(1): 37-47 (in Chinese).
[30] LIU Yu-bao, ZHANG Da-lin, YAU M K. A multiscale numerical study of Hurricane Andrew (1992) Part I: Explicit simulation and verification [J]. Mon Wea Rev, 1997, 125(12): 3073- 3093.
[31] BRAUN S A, TAO W K. Sensitivity of high-resolution simulations of Hurricane Bob (1991) to planetary boundary layer parameterizations [J]. Mon Wea Rev, 2000, 128(12): 3941-3961.
[32] DAVIS C A, BOSART L F. Numerical simulations of the genesis of Hurricane Diana (1984) Part II: Sensitivity of track and intensity prediction [J]. Mon Wea Rev, 2002, 130(5): 1100-1124.

Citation: WANG Li-juan, DAI Zhu-jun and HE Jie-lin. Numerical simulation of the relationship between the maintenance and increase in heavy rainfall of the landing tropical storm Bilis and moisture transport from lower latitudes [J]. J Trop Meteorol, 2017, 23(1): 47-57.